MODEL OF A NUCLEAR THERMAL TEST PIPE USING ATHENA

THESIS

Mark J. Dibben, Captain, USAF

AFIT/GNE/ENP/92M-2

DEPARTMENT OF THE AIR FC
AIR UNIVERSITY
AIR FORCE INSTITUTE OF TECHNOLOGY

Wright-Patterson Air Force Base, Ohio

AFIT/GNE/ENP/92M-2

MODEL OF A NUCLEAR THERMAL TEST PIPE USING ATHENA

THESIS

Mark J. Dibben, Captain, USAF

AFIT/GNE/ENP/92M-2

Approved for public release: distribution unlimited

REPORT DOCUMENTATION PAGE

Form Approved
OMB No. 0704-0188

1. AGENCY USE ONLY (*Leave blank*)

2. REPORT DATE
March 1992

3. REPORT TYPE AND DATES COVERED
Master's Thesis

4. TITLE AND SUBTITLE
MODEL OF A NUCLEAR THERMAL TEST PIPE USING ATHENA

5. FUNDING NUMBERS

6. AUTHOR(S)
Mark J. Dibben, Captain, USAF

7. PERFORMING ORGANIZATION NAME(S) AND ADDRESS(ES)
Air Force Institute of Technology, WPAFB OH 45433-6583

8. PERFORMING ORGANIZATION REPORT NUMBER
AFIT/GNE/ENP/92M

9. SPONSORING/MONITORING AGENCY NAME(S) AND ADDRESS(ES)
MARLAND L. STANLEY
EG&G IDAHO, INC
P.O. BOX 1625
Idaho Falls ID 83415

10. SPONSORING/MONITORING AGENCY REPORT NUMBER

11. SUPPLEMENTARY NOTES

12a. DISTRIBUTION/AVAILABILITY STATEMENT
Approved for public release; distribution unlimited

12b. DISTRIBUTION CODE

13. ABSTRACT (*Maximum 200 words*)

Nuclear thermal propulsion offers significant improvements in rocket engine specific impulse over rockets employing chemical propulsion. The computer code ATHENA (Advanced Thermal Hydraulic Energy Network Analyzer) was used in a parametric analysis of a fuelpipe. The fuelpipe is an annular particle bed fuel element of the reactor with radially inward flow of hydrogen through it. The outlet temperature of the hydrogen is parametrically related to key effects, including the effect of reactor power at two different pressure drops, the effect of the power coupling factor of the Annular Core Research Reactor, and the effect of hydrogen flow. Results show that the outlet temperature is linearly related to the reactor power and nonlinearly to the change in pressure drop. The linear relationship at higher temperatures is probably not valid due to dissociation of hydrogen. Once thermal properties of hydrogen become available, the ATHENA model for this study could easily be modified to test this conjecture.

14. SUBJECT TERMS
Nuclear Propulsion, Nuclear Reactors, ATHENA, Propulsion Systems, Computerized Simulation

15. NUMBER OF PAGES
72

16. PRICE CODE

17. SECURITY CLASSIFICATION OF REPORT	18. SECURITY CLASSIFICATION OF THIS PAGE	19. SECURITY CLASSIFICATION OF ABSTRACT	20. LIMITATION OF ABSTRACT
Unclassified	Unclassified	Unclassified	UL

AFIT/GNE/ENP/92M-2

MODEL OF A NUCLEAR THERMAL
TEST PIPE USING ATHENA

THESIS

Presented to the Faculty of the School of Engineering
of the Air Force Institute of Technology
Air University
In Partial Fulfillment of the
Requirements for the Degree of
Master of Science in Nuclear Engineering

Mark J. Dibben, B.S.
Captain, USAF

March 1992

Preface

The purpose of this study was to develop a simulation of a fuelpipe using the computer code ATHENA. It originally started out as a short research project but the installation of the program took more than half of the quarter.

Thanks are in order to my faculty advisor, Col Tuttle, for allowing me to continue to work on this project even after he left this organization. Dr. Elrod was also helpful in obtaining information for me concerning properties of hydrogen.

I would also like to thank several people at INEL for the assistance they have given me on this project. Dick Wagner successfully installed ATHENA after we had failed and helped me with parts of the programming. Tony Zuppero answered questions for me concerning the project and found other people at INEL to help me.

Final thanks go to my family. Jason, Luis, and Amanda have been an inspiration and deserve lots of my time now that this is finished.

Table of Contents

List of Figures

List of Tables

Abstract

Nuclear thermal propulsion offers significant improvements in rocket engine specific impulse over rockets employing chemical propulsion. The computer code ATHENA (Advanced Thermal Hydraulic Energy Network Analyzer) was used in a parametric analysis of a fuelpipe. The fuelpipe is an annular particle bed fuel element of the reactor with radially inward flow of hydrogen through it. The outlet temperature of the hydrogen is parametrically related to key effects, including the effect of reactor power at two different pressure drops, the effect of the power coupling factor of the Annular Core Research Reactor, and the effect of hydrogen flow. Results show that the outlet temperature is linearly related to the reactor power and nonlinearly to the change in pressure drop. The linear relationship at higher temperatures is probably not valid due to dissociation of hydrogen. Once thermal properties of hydrogen become available, the ATHENA model for this study could easily be modified to test this conjecture.

MODEL OF A NUCLEAR THERMAL TEST PIPE USING ATHENA

I Introduction

1.1 Background

In 1989 the President Bush proposed the Space Exploration Initiative (SEI). This proposal called for astronauts to return to the Moon and to go to Mars early in the 21st century. To develop this proposal, Vice President Quayle and National Aeronautics and Space Administration administrator Richard H. Truly formed the Synthesis Group whose goal was to study ideas and suggestions for America's space program (Synthesis Group, 1991:86). Their recommendations call for the development of both the nuclear thermal rocket and space nuclear power technologies. The nuclear thermal rocket can be used to reduce the travel time to Mars from the estimated 450-500 days for chemical rockets to only 120-180 days. This reduced travel time will help to minimize the astronauts exposure to solar and galactic radiation (Asker, 1991b:39 2 Dec). Boeing Space & Defense Group has also analyzed different propulsion systems for spacecraft to Mars and has determined that nuclear thermal is better than

chemical, solar electric, or nuclear electric propulsion (Asker, 1991a:24 18 Mar 1991).

The manned mission to Mars is not the only use for the nuclear thermal rocket. Ramsthaler and Sulmeisters (1988:21) have determined that among nuclear thermal, chemical, and nuclear electric, the direct-thrust nuclear stage is the most cost effective propulsion system for performing the LEO (Low Earth Orbit) to GEO (Geosynchronous Earth Orbit) orbit transfer mission. They have concluded that the direct thrust nuclear rocket engine should be the priority Air Force development system for orbital maneuvering and transfer mission.

Particle Bed Reactors (PBR) are the power source in nuclear thermal rockets. Lazareth and others (1987:223) outline four objectives PBR's meet that allow them to potentially power space-based weapon systems as well. They can be integrated into Strategic Defense Initiative weapons, they can deliver full power in just a few seconds, they can operate at hundreds to thousands of megawatts of power, and finally they can operate for hundreds to thousands of seconds. These characteristics are ideal for space-based weapons.

1.2 Problem and Scope

Idaho National Engineering Laboratory has been contracted by the Air Force Astronautical Laboratory as the overall program manager for the development of the nuclear engine (Ramsthaler and Sulmeisters, 1988:19). During this program, INEL has asked AFIT to make a computer simulation of one part of this nuclear thermal rocket, a fuelpin. The purpose of this thesis is to model this fuelpin and to determine the thermal hydraulic flow characteristics within it. The computer code ATHENA (Advanced Thermal Hydraulic Energy Network Analyzer) will be used to make this simulation.

1.3 Particle Bed Reactor

The fuelpin that will be modeled is one element of a particle bed reactor. It consists of small fuel particles confined in an annulus between two concentric frits (Figure 1). The fuel particles are made of a uranium carbide kernel surrounded by a layer of graphite and coated with zirconium carbide to prevent chemical reactions with hydrogen. Hydrogen flows radially inward through the fuel bed and is then exhausted axially through the channel formed by the inner frit. The porosity of the outer, or cold frit, can be varied axially to maintain a uniform temperature along the inner or hot frit. By changing the porosity of the frit,

the hydrogen mass flow rate is changed. This is necessary because of variations in the shape of the power curve (Benenati and others, 1987:139).

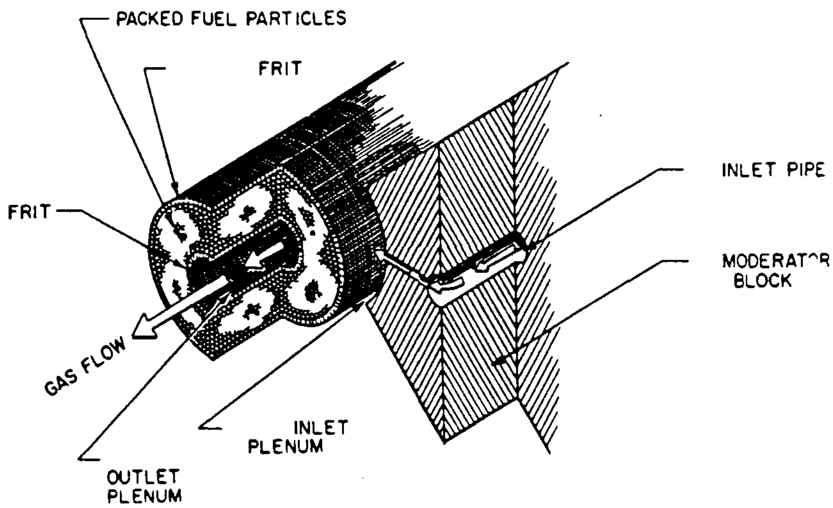

Figure 1. Diagram of Fuelpin (Lazareth, 1987:225)

1.4 Nuclear Thermal Rocket

One design for a nuclear thermal rocket uses 19 of these fuel elements arranged in a moderator. After the propellant flows through the fuel elements, it is then ejected through the rocket nozzle. An indicator of rocket engines is the specific impulse. It is proportional to the square root of the gas temperature at the nozzle inlet and inversely proportional to the square root of the molecular weight of the exhaust gas. To increase the specific impulse, the

propellant temperature must be increased and the molecular weight of the propellant decreased. For most systems, this implies a hydrogen propellant operating at as high of temperature as possible (Araj and others, 1988:85). In a particle bed reactor, the highest temperatures are seen in the innermost part of the fuel bed, the hot frit and the exhaust channel. Therefore, the temperature is limited by the materials these sections are made of. If halfnium is substituted for zirconium in these high temperature areas, the maximum temperature can be raised to 3600 K instead of 3200 K for zirconium materials (Leyse and others, 1990:2).

The specific impulse for chemical engines is about 500 seconds while some low pressure nuclear thermal rockets have analytically reached over 1250 seconds. The dissociation of hydrogen is attributed with some of this increase in specific impulse, but because of uncertainties in the kinetics of hydrogen dissociation/recombination, its contribution may be questionable (Leyse and others, 1990a:2). However, even without the benefits of dissociation, the specific impulse offered by nuclear thermal rockets is much greater than any achieved by chemical rockets.

1.5 Literature Review

RELAP5 (Reactor Excursion and Leak Analysis Program) is the code from which ATHENA is derived. A review of the lit-

erature found no other RELAP5 models similar to a particle bed reactor. The primary use of RELAP5 is in modeling light water reactors for loss of coolant accidents and other transient failures. When the ATHENA code became available three other models of a similar nature to this project were found. Two of these modeled the SP-100 (Fletcher, 1986:Chapter 10 and Roth, 1987:Chapter 46). One other model simulated a simplified version of a fuelpipe (Roth, unpublished).

The review also found a lack of property data for the materials used in a particle bed reactor. Specifically, thermal properties for ZrC and UC_2 were not found above 2800-3000K while this project required data to at least 3200 K and possibly to 3600 K. Heat capacities were available for ZrC to 3000 K and for UC to 2800 (Storms, 1967:29, 201). A secondary source listed thermal conductivity data for ZrC to 3000 K and for UC_2 to 3200 K (Smalec, 1990:99, 103), while a primary source listed data to only 2100 K for UC and 2700 for ZrC (Touloukian and others, 1970:109, 609).

The same data was required for pyrolytic graphite. The value of these properties varied up to two orders of magnitude depending on the density and direction of propagation of heat (Touloukian and others, 1970:30-31, 41). More specific information regarding these materials is needed to ensure proper treatment.

Hydrogen property data is also lacking. It is known

that hydrogen dissociates as the temperature is increased and the dissociation becomes even greater as the pressure is decreased as shown in Figure 2. At 20 atmospheres dissociation begins at 2800 K and is ten percent dissociated by 3500 K. This range also happens to be the operating range for a nuclear thermal rocket. This dissociation will change the thermal properties of hydrogen allowing it to carry away more heat from the fuel. This additional heat capacity of the hydrogen lowers the temperature in the core, thus permitting the reactor to operate at a higher power. Dissociation will also increase the pressure of the hydrogen by increasing the number of molecules which in turn will increase the specific impulse of a rocket. Although all of this is known, the property data is not available to allow adequate modeling. INEL has initiated an experiment for providing this needed data (Leyse, 1990b:1), but it is not yet available. As a result, modeled outlet temperatures from the reactor will exceed actual temperatures in most cases.

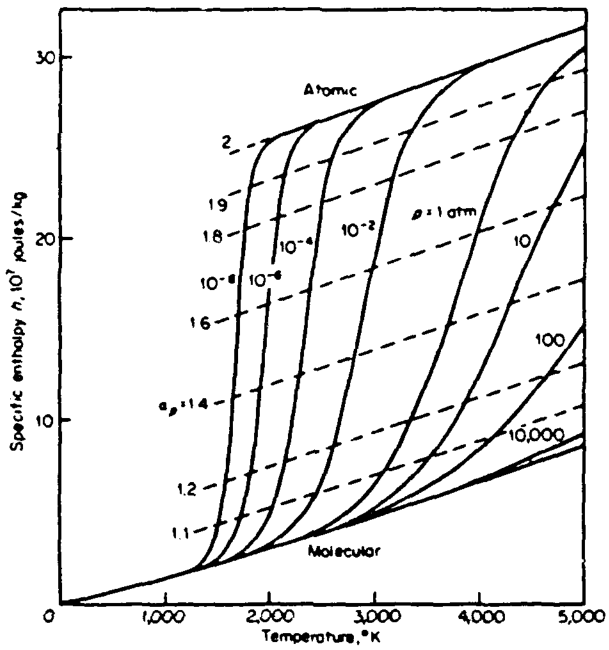

Figure 2. Dissociation of Hydrogen (Jahn, 1968:97)

II The ATHENA Code

The RELAP5 (Reactor Excursion and Leak Analysis Program) computer code was developed at the Idaho National Engineering Laboratory (INEL) for the U. S. Nuclear Regulatory Commission (NRC). The ATHENA code is an expanded version of the RELAP5 code, which has become an industry standard for light water reactors. It can be used to model the thermal hydraulics of complete energy generation and/or conversion systems at normal operating conditions and during off-normal transients (Roth, undated:1).

2.1 RELAP5 Code Description

The RELAP5 code is based on a nonhomogeneous and non-equilibrium model for the two-phase system that is solved by a fast, partially implicit numerical scheme to permit economical calculation of system transients . The code includes many generic models that are used as the basic structure to make more complex systems. These models include pumps, valves, pipes, heat structures, reactor point kinetics, electric heaters, jet pumps, turbines, separators, accumulators, and control system components. Because of limited knowledge of systems and because of finite computer resources, many approximations are used in the code. For example, two phase flow is not fully understood. Also, items such as spatial nodalization are required to be of a

finite size. It is not possible to calculate the pressure at every single point along a pipe. The approximations used in this code are necessary to model real systems and allow them to be solved in a reasonable amount of time (Carlson and others, 1990:iv, 1-5).

Generally, modeling a system with RELAP5 is divided into two sections - hydrodynamics and heat flow. The hydrodynamic model is based on the use of fluid control volumes and junctions that represent the actual flow of fluid in the system. Control volumes are connected together with junctions at the inlet and outlet to model the flow path of the fluid. Fluid scalar properties such as pressure, energy and density are averaged over the entire cell volume and located at the center of the control volume. Vector properties such as fluid velocities are located at the junctions.

Heat flow models are used to represent heat structures such as pipe walls, heater elements, nuclear fuel pins and heat exchanger surfaces. Heat structures are thermally connected to the hydrodynamic control volumes. For example, if the wall of a pipe could exchange heat with the fluid flowing within it. the pipe wall would be connected to the control volume of fluid.

Neither RELAP5 nor ATHENA currently have graphics capability. However, during a simulation, information can be saved at certain time intervals to a plot file. A small

program is then used to create a strip file, shown in Appendix A, to extract information used in making graphs. This strip file was then modified with another program, shown in Appendix B, to create files that can be read by programs such as TK or Freelance.

2.2 Expanded Capabilities of ATHENA

The major difference between RELAP5 and ATHENA is ATHENA's ability to model working fluids other than water. These include hydrogen, helium, lithium, sodium and potassium. Two eutectic liquid fluids are available: LiPb (17 atom percent lead) and NaK (22.2 weight percent sodium). ATHENA can also be modified to specify any acceleration due to gravity. Normally, it is set to the earth's surface value but it can also be set to zero for space applications. It is because of the features of RELAP5 and the upgrades to ATHENA that this code was selected for this project.

III Modeling of the Fuelpipe

3.1 Availability of data

The primary source of information used for making this simulation was obtained from L. M. Smalec's technical data record (Smalec, 1990). In some cases, because of a lack of information, certain assumptions had to be made. These and all other aspects of the simulation will be documented as they are presented. This simulation models an experimental setup but is not compared to any data because it was not available at the time of this work.

3.2 Layout of the Volumes

For this simulation, it was chosen to divide the fuel-pipe into five regions axially and seven regions radially, one section in the inlet channel, five sections in the fuel bed and one section in the exhaust channel as shown in Figure 3. This was done to adequately represent the change in temperature and pressure through the fuelbed. Volumes 60 and 62 represent boundary conditions. The hydrogen enters from volume 60 and flows into the inlet channel, volumes 1-5. It then flows radially through the fuel bed, volumes 6-30. The heated hydrogen is exhausted through volumes 31-35 to the outlet boundary condition, volume 62. Junctions connect each of the volumes both radially and axially

to include cross flow within the fuelbed. A total of 37 hydrodynamic volumes and 60 junctions are required to be modeled.

The measurements and characteristics assumed for this fuelpipe are shown in Table 1. These physical characteristics of the fuelpipe must be translated into a format readable by ATHENA. This is done by creating an input deck. This input deck contains the geometry of the hydrodynamic volumes, areas of junctions connecting the volumes, initial input status, heat structure data including thermal properties of all materials used in the system and finally, the power table. A typical input deck is shown in Appendix C.

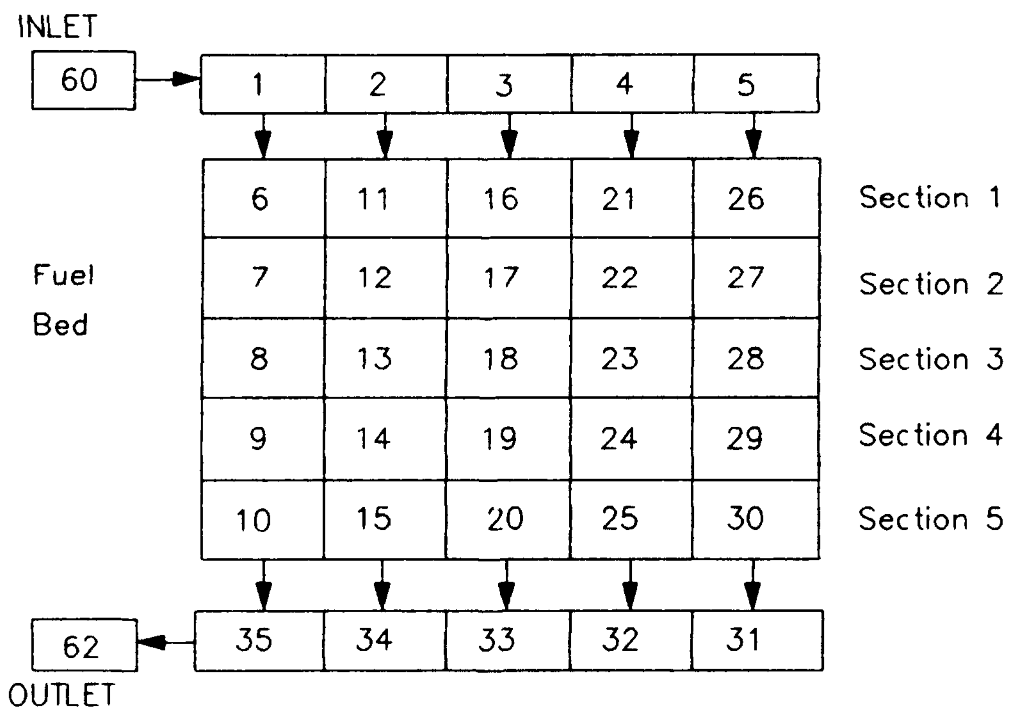

Figure 3. Layout of Fuel Volumes

Table 1.

Fuelpipe Parameters

Length of active bed	25.4 cm
Outlet plenum id	2.85 cm
hot frit thickness	0.15 cm
cold frit id	5.50 cm
cold frit thickness	0.51 cm
inlet plenum od	8.92 cm
coupling factor to ACRR	33.0 W/MW/cm^3
fuel bed volume	428.5 cm^3
fuel pellet	
Uranium carbide od	0.240 mm
LTI od	0.304 mm
pyrolytic graphite od	0.404 mm
zirconium carbide od	0.500 mm
void fraction	0.36

3.2.1 Modeling of the Hydrodynamic Volumes The major consideration in modeling the hydrodynamic volumes is the geometry. Based on the dimensions previously shown in Table 1, the volumes were divided equally in the axial direction. They were also divided radially so as to have the same radial length. The calculation of the volume of the hydrodynamic volume is based on the space occupied by the hydrogen. This excludes any space occupied by the fuel particles. Therefore, the actual volume of hydrogen is found by multiplying by the void fraction of 0.36. The flow area is also affected by the fuel particles. The corrected volume divided by the radial length of each cell gives the flow area so that each hydrodynamic volume is consistent in

its dimensions.

Friction factors were calculated for the flow through the packed bed. This is based on the equation

$$K = \frac{\Delta P 2 g_c \rho A^2}{\dot{m}}$$

K = flow energy loss coefficient

g_c = gravitational constant

ρ = density of hydrogen

A = flow area

$\dot{m}$ = mass flow rate of hydrogen

It was found that this factor was nearly constant for varying flow rates.

One point of departure from the technical data record is the hydraulic diameter. It is listed as 500 µm, the diameter of the fuel par+icles. Another reference (Bennett, 1982:212) equates the hydraulic diameter for flow through a packed bed to the following equation

$$r_H = \frac{1}{6}\frac{\epsilon}{(1-\epsilon)}D$$

r_H = hydraulic radius

ϵ = void fraction

D = diameter of particle

The hydraulic diameter is then twice the hydraulic radius. This yields a hydraulic diameter of 93.8 μm. This value has been used in all subsequent calculations.

3.2.2 Modeling of the Heat Structures More work was required to determine the needed parameters for the heat structures. The primary heat structure is the fuel. It is thermally linked to the hydrodynamic volumes (hydrogen). The assumed power distribution is shown is Table 2. The numbers represent relative power levels. Axially, the power is lower on the ends and increases towards the middle. Because each radial section has decreasing volume as it approaches the inside of the annulus, the power also decreases radially inward.

Table 2

Power Distribution

		Axial 1	2	3	4	5
Radial	1	1.4685	1.6355	1.6895	1.6482	1.5083
	2	1.0963	1.2210	1.2613	1.2304	1.1260
	3	0.8506	0.9473	0.9787	0.9547	0.8737
	4	0.6715	0.7478	0.7725	0.7536	0.6896
	5	0.5311	0.5914	0.6110	0.5960	0.5454

ATHENA requires heat capacity and thermal conductivity data for all heat structure materials for the entire range of encountered temperatures. As mentioned previously, much

of this data is not available. The lack of accurate data is a serious deficiency in this simulation. Where possible, existing data has been extrapolated to cover the range of interest. Because of the large variation in the thermal properties for graphite, a constant value for heat capacity and thermal conductivity were used.

The fuel pipe was powered by being brought into contact with the Annular Core Research Reactor (ACRR). The power scaling factor between the ACRR and fuelpipe is determined by

$$\text{Power scaling factor} = \text{coupling factor} \times \text{bed volume}$$

The coupling factor is assumed to be 33 $W/MW/cm^3$, while the bed volume is fixed at 428.5 cm^3. By multiplying this factor by the ACRR power, the total power being developed in the bed is calculated.

3.2.3 Boundary Conditions The area of interest for this project was the fuelpipe itself. By concentrating on this the rest of the nuclear thermal rocket was ignored. What happened to the hydrogen gas before it reached the inlet to the fuelpipe was ignored. Therefore, initial conditions were set at the inlet of the pipe to specify the temperature

and pressure of the hydrogen. Specifying the pressure at the outlet boundary condition designates the pressure drop across the entire pipe. Because of forward flow, the suggested outlet temperature was inconsequential since the temperature of the previous volume is the outlet temperature. Given the inlet and outlet pressures, pressure drops across all boundaries are also specified. This also determines the flow rate of hydrogen throughout the system.

IV Results and Discussion

The specifications for the baseline case that was used as a reference for this study are outlined in Table 3. The parameters that were individually studied are ACRR power at two different pressure drops, the coupling factor and the flow rate of hydrogen.

4.1 Base Case

Using the conditions of Table 3, the temperature of the hydrogen gas was calculated as it exits the fuelpipe. This is presented in Figure 4 as a function of time. It is clear that the maximum temperature of 804 K has been reached within five seconds. This same equilibrium time was observed in all of the other simulations. It also compares very well to results obtained by Lazareth and others (1987:225). Using a different program, they obtained maximum reactor coolant temperature in 4.4 seconds. This short equilibrium time allows the computer simulations to be completed within twenty four hours on the Sun workstations making a parametric study possible. Unless otherwise noted, all outlet temperatures will be based on this five second period.

Table 3

Initial Conditions for Base Case

Inlet H_2 temperature	300 K
Inlet H_2 pressure	2.068 MPa
Outlet H_2 pressure	2.02 MPa
ACRR Power	16 MW
Coupling Factor	33 W/MW/cm^3

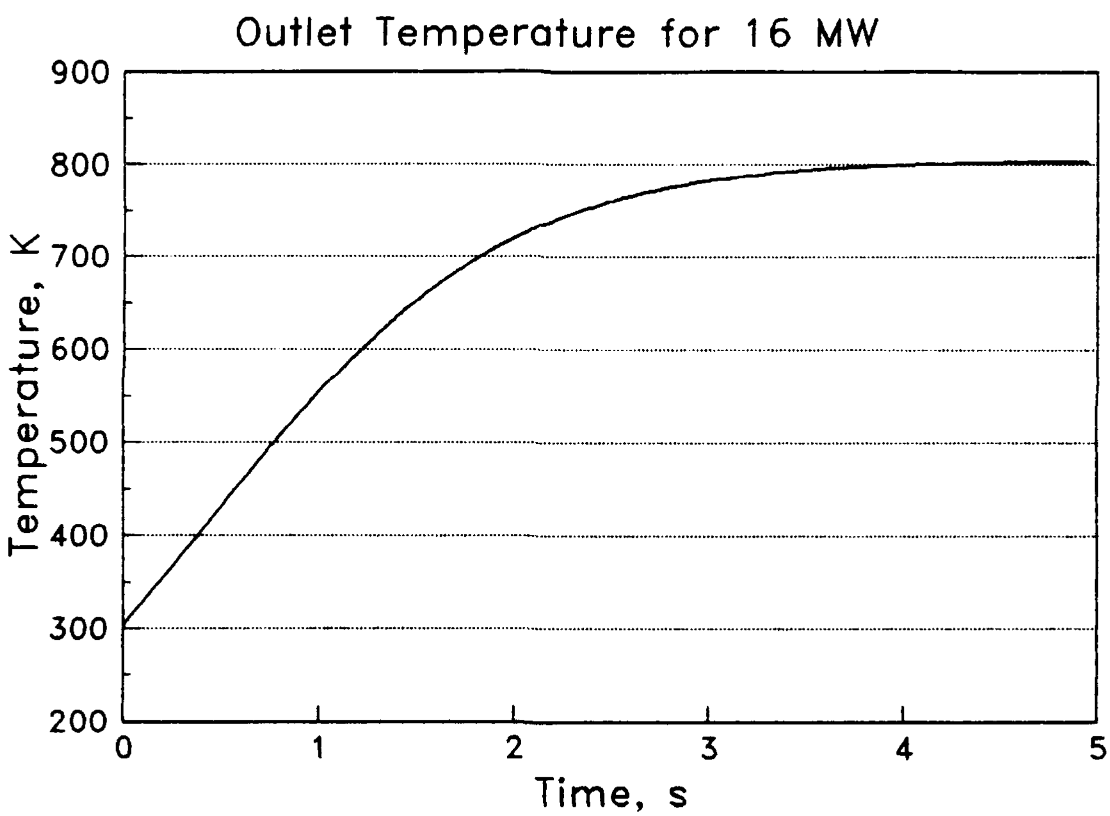

Figure 4. Outlet Temperature for Base Case

Since the fuelbed has been divided into 25 hydrodynamic volumes, the average temperature of the hydrogen can be found in each of these volumes. Figure 5 tracks this average

temperature as the hydrogen flows radially inward for each of the five axial sections.

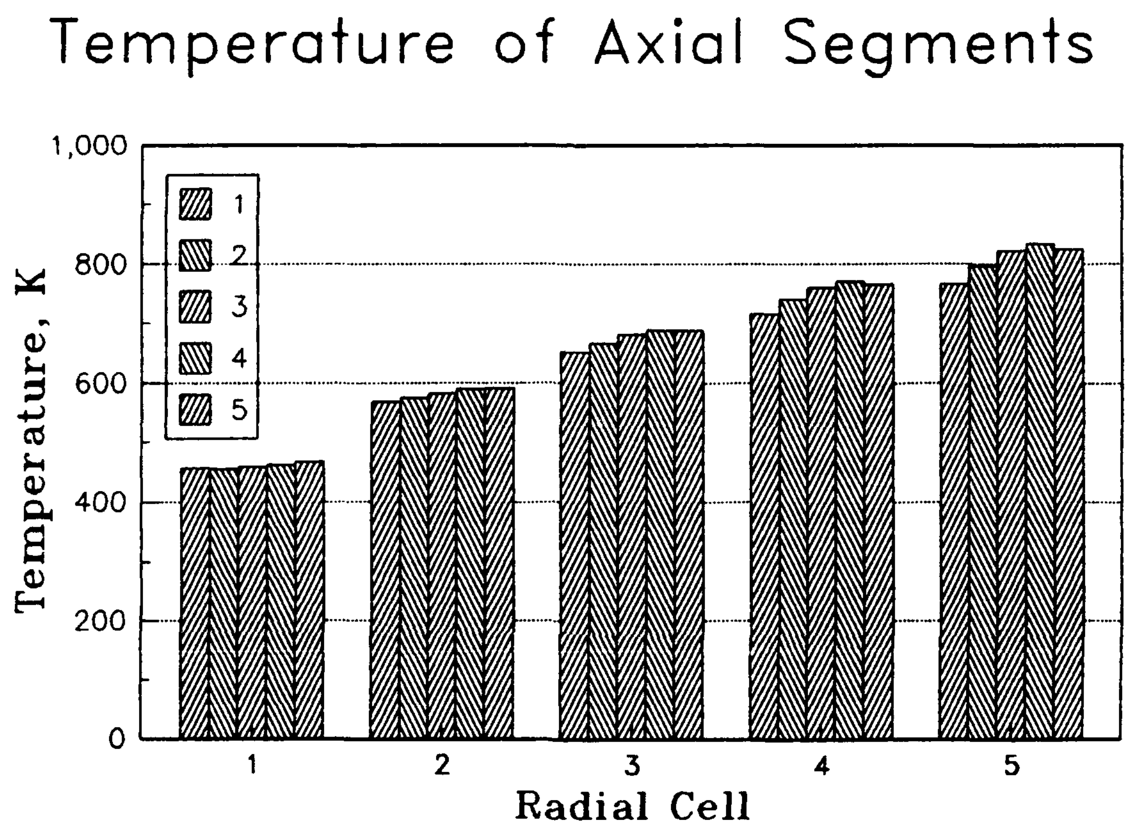

Figure 5. Temperature Profile of Base Case

Each line represents one axial section. The maximum temperature is at the innermost radial section. However, this innermost temperature is not the same for each section. It is highest for section four and lowest for section one, the section nearest the inlet. This inequality is indicative of the nonuniform power distribution through the fuel bed. This could be improved by adjusting the flow rate of

hydrogen. This is accomplished by varying the porosity of the cold frit. At the inlet, the frit could be made less porous thus decreasing the flow rate and increasing the temperature. Likewise, it could be made more porous at the center and lower the temperature in those sections.

As the hydrogen flows through the fuel bed, its velocity increases as it is heated. The velocity of the hydrogen ranges from 0.35 m/s at the outer edge of the fuelbed to 1.7 m/s as it reaches the hot frit.

4.2 Constant Pressure Drop

The first parameter studied was the effect of reactor power on the outlet temperature while the fuelpipe maintained a constant pressure drop. As in the baseline case, the inlet pressure was maintained at 2.068 MPa and the outlet pressure was 2.02 MPa. This pressure drop allowed a hydrogen flow rate of approximately 0.03 kg/s. As the reactor power increased, this flow rate dropped slightly but all flow rates were within 10% of this value. Figure 6 shows the outlet temperature as the reactor power varies from 2 MW to 84 MW. This figure clearly shows a linear relationship between reactor power and outlet temperature. However, the thermal property data generated by the ATHENA code is valid only to 1800 K (Tolli, 1991). Even if the values generated by ATHENA approximate those of an ideal gas at the higher

temperatures, hydrogen begins to depart from this. Dissociation begins at 2800 K for this pressure and increases as the temperature increases (Jahn, 1968:97). Because of these difficulties, the rest of this study will be limited to cases with outlet temperatures below 1800 K. For any future study to be meaningful, data for ranges up to 3500 K will be required.

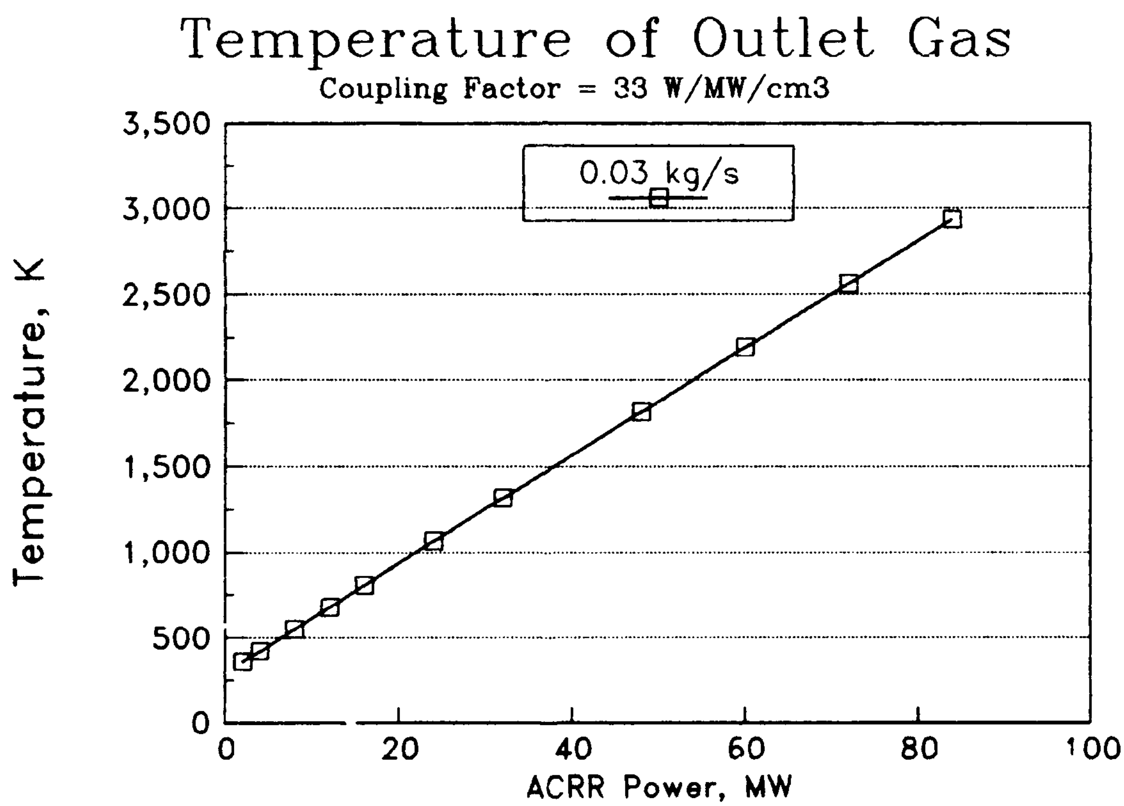

Figure 6. Temperature Comparison at Low Flow

4.3 Higher Pressure Drop

The same reactor power levels were next examined with a larger pressure drop across the pipe. The inlet pressure was kept at 2.068 MPa while the outlet pressure was dropped from 2.02 MPa to 1.85 MPa. This produced a hydrogen flow rate of approximately 0.065 kg/s. While the pressure drop increased by 4.5 times, the mass flow rate only slightly more than doubled. The outlet temperatures for different reactor levels are shown in Figure 7.

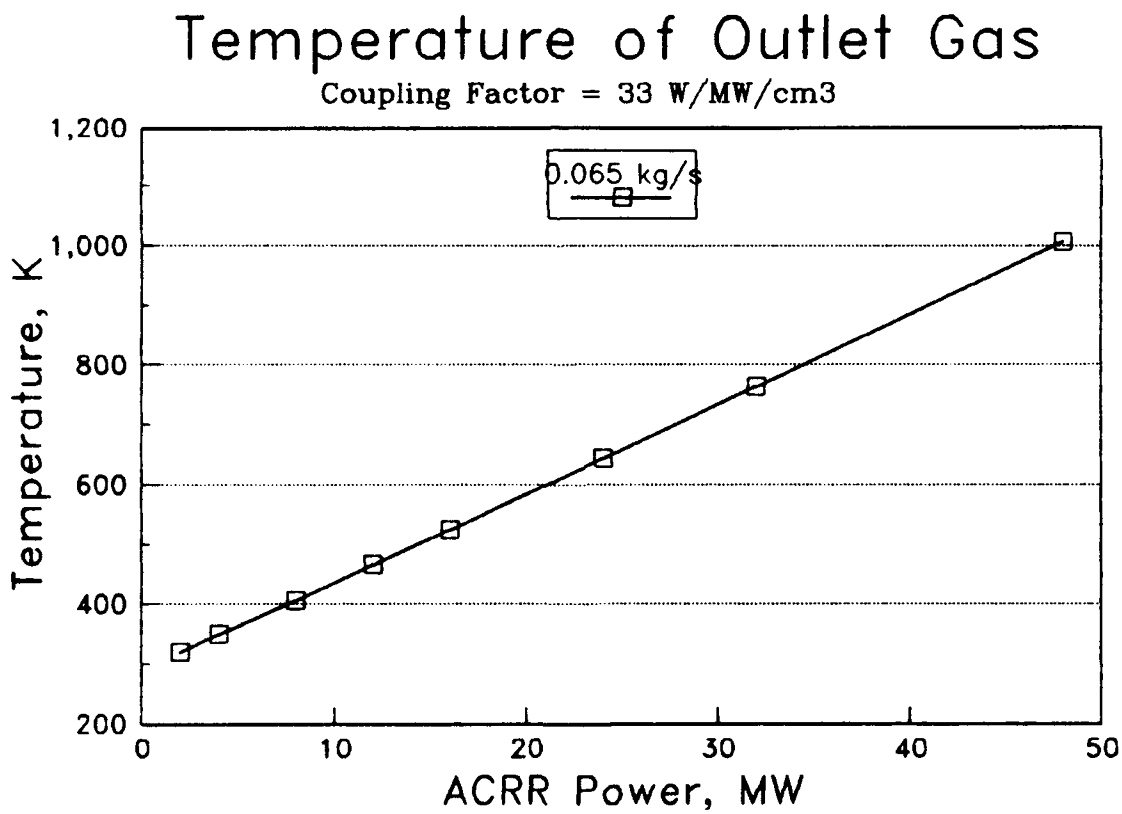

Figure 7. Temperature Comparison at High Flow

The same linear relationship is seen in this figure as in that of the lower flow rate. The only difference is a lower outlet temperature. A direct comparison is shown in Figure 8. Remembering that the initial inlet temperature is 300 K, there is little difference at the lower power levels but this difference is clear at the higher power levels.

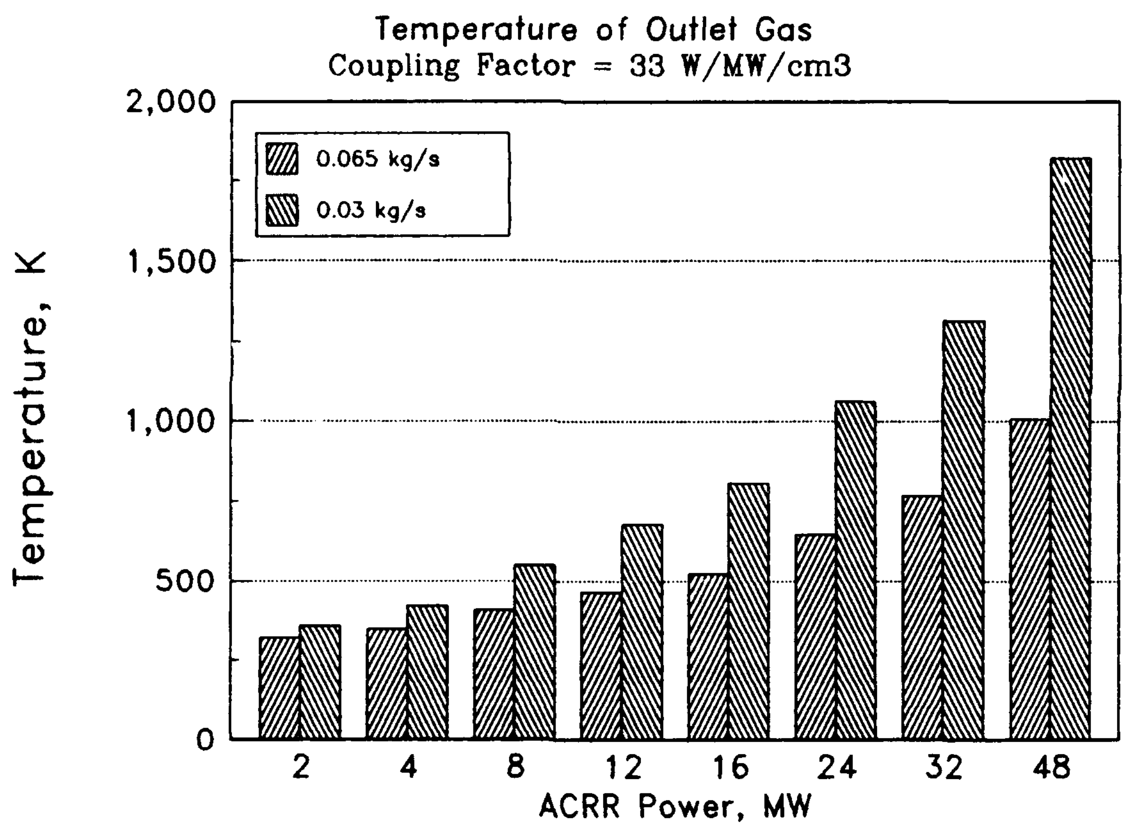

Figure 8. Comparison of Outlet Temperatures at Both Flow Rates

4.4 Coupling Factor

The coupling factor was initially assumed to be 33 W/MW/cm^3. Assuming the ACRR power level is 16 MW, then 0.23 MW is developed in the fuelpipe (ACRR power x coupling factor x bed volume). By changing the coupling factor, a different power level is assumed to be developed in the fuelpipe. Table 4 shows the different outlet temperatures reached with coupling factors of 30, 33 and 36 W/MW/cm^3. By changing the coupling factor 9%, the outlet temperature changes by only 6%. The change is linear since the same effect could be observed by changing the ACRR power the same amount. However, this does show that the outlet temperature is somewhat sensitive to some of the initial assumptions.

Table 4

Observed Outlet Temperature for

Change in Coupling Factor

Coupling Factor	Outlet Temperature
30	757.6
33	804.4
36	851.0

4.5 Mass Flow Rate

The final parameter studied was the mass flow rate. This is related to the variation in the pressure drop but it was earlier shown that this is not a one to one relationship. The inlet pressure was held constant at 2.068 MPa and the outlet pressure was varied from 1.80 MPa to 2.04 MPa at a constant ACRR power of 16 MW. Figure 9 shows the effect of pressure drop on the hydrogen flow rate. Flow rate is clearly not a linear function of pressure drop. As the pressure drop increases, a greater change is required to obtain the same change in hydrogen flow rate.

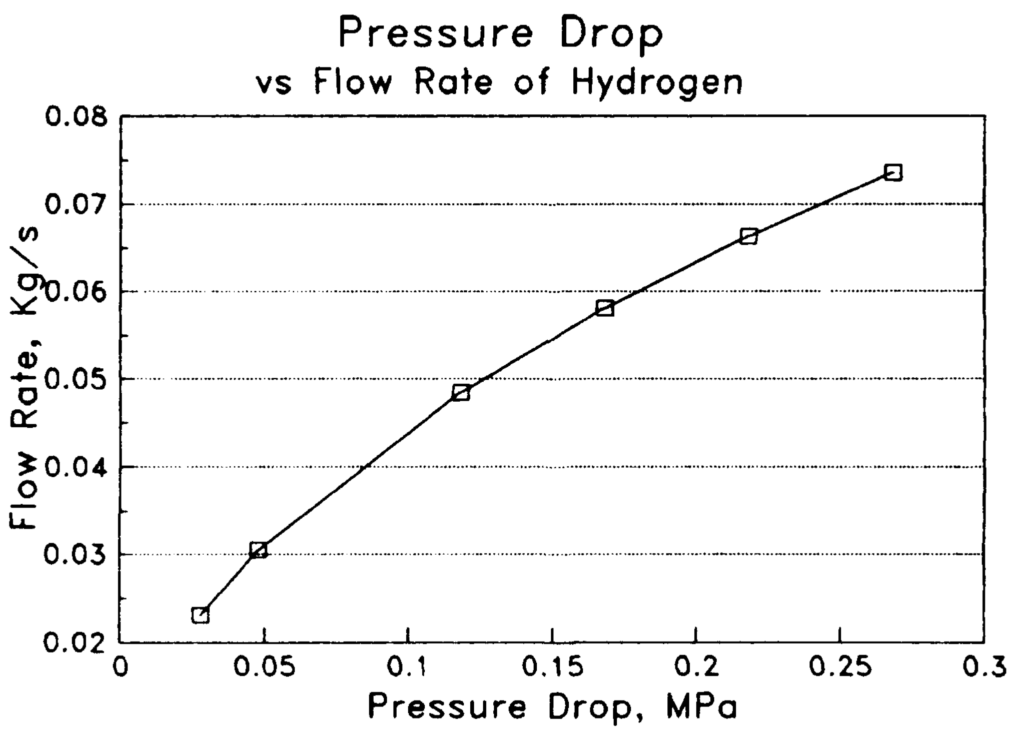

Figure 9. Pressure Drop vs. Flow Rate

The hydrogen cross flow or the flow of hydrogen axially instead of radially was also examined. This cross flow occurs because of pressure differences in the pipe caused by nonuniform heating. Figure 10 shows the maximum cross flow occurs in the outermost radial section which is shown as the first group of bars. Each bar represents the flow between neighboring axial volumes. The negative value for the fourth junction indicates flow going the opposite direction. As the hydrogen flows radially inward, there is less cross flow. It was found that this cross flow varies between one tenth and one percent of the radial flow with the average being three tenths of one percent. As mentioned previously, a non-uniform cold frit could be used to vary the radial flow to obtain a constant outlet temperature. While hydrogen cross flow will occur, its small value should not completely counter-act the use of the cold frit.

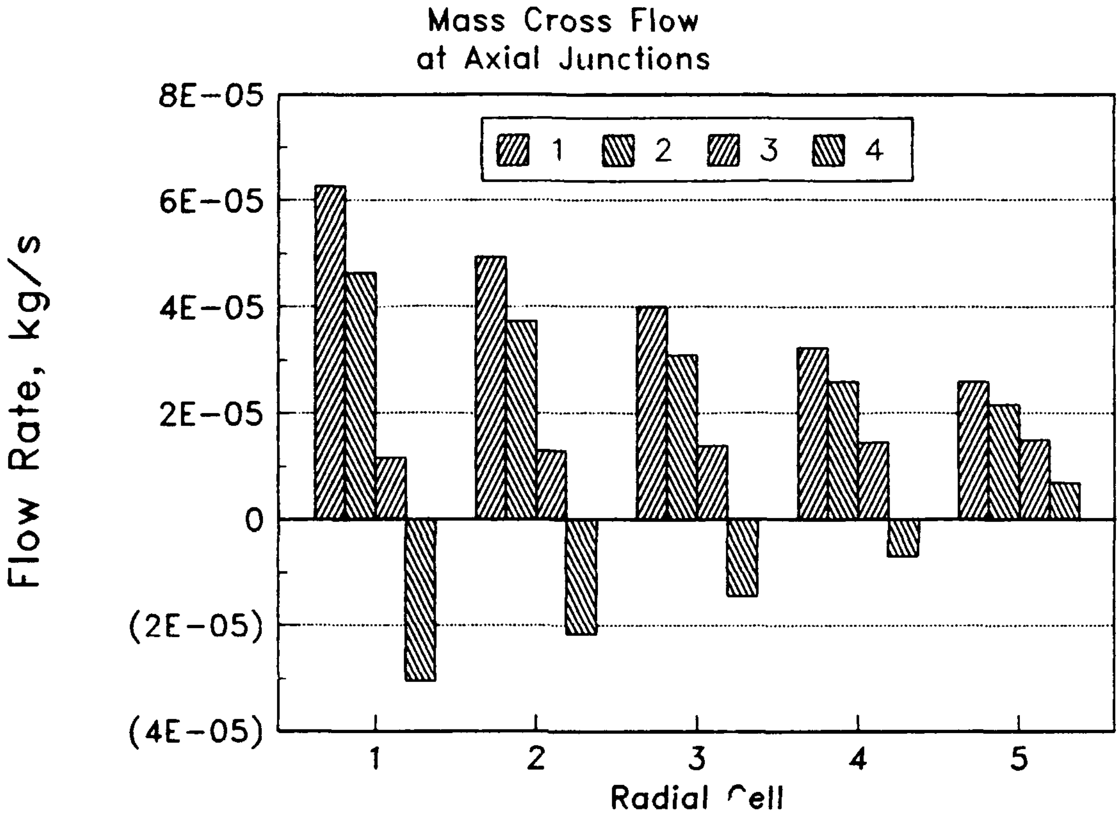

Figure 10. Mass Cross Flow at Axial Junctions

It has been shown that the outlet temperature changes linearly with the hydrogen flow rate. Therefore, it is expected the outlet temperature will be nonlinear with respect to pressure drop as was the hydrogen flow rate. This is shown in Figure 11.

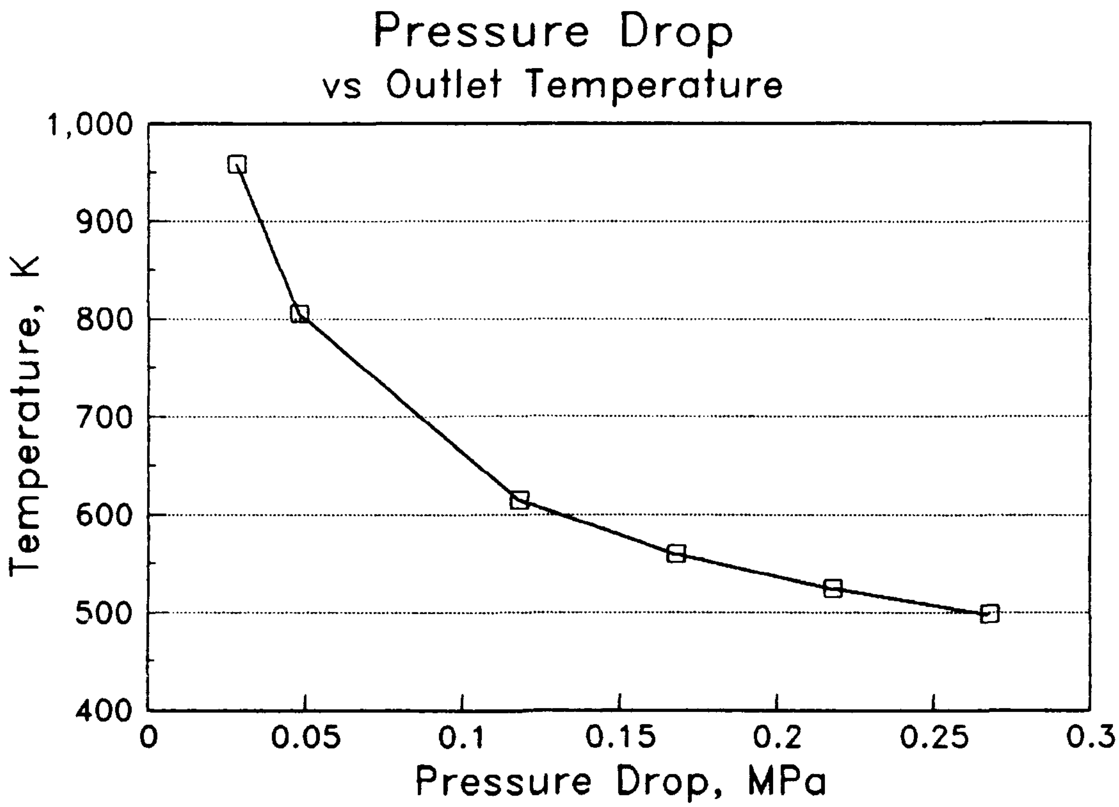

Figure 11. Outlet Temperature vs. Flow Rate

V Conclusions and Recommendations

It is clear the temperature of the outlet gas is linearly related to the power generated in the particle bed reactor. However, at temperatures above 2800 K, this relation is questioned. Without more complete data concerning the dissociation of hydrogen, further simulations will be meaningless.

The fuelpipe reaches thermal equilibrium within five seconds. This short equilibrium time allows computer simulations to be completed within a reasonable time of twenty four hours.

It was also found that hydrogen flow rate and thus outlet temperature, is not linear with the pressure drop across the fuelpipe. As the pressure drop increases, a smaller increase in hydrogen flow is realized.

The crossflow or axial flow of hydrogen in the fuelpipe averaged just three tenths of one percent of the radial flow. This minimal cross flow should not counter-act the use of a non-uniform cold frit to obtain constant outlet temperatures.

The input deck that has been produced by this thesis work is a starting point for modeling any other fuel pipes. With added information, this could be very useful in simulating the thermal hydraulic characteristics of any fuelpipe.

Appendix A: Graphics Strip Program

```
*This program strips specific data from the run file and
*puts it into a usable format.
*
=fuel strip problem
0000100 strip fmtout
103 0
1002 tempg 060010000
1003 tempg 001010000
1004 tempg 002010000
1005 tempg 005010000
1006 tempg 006010000
1007 tempg 010010000
1008 tempg 011010000
1009 tempg 015010000
1010 tempg 016010000
1013 tempg 025010000
1015 tempg 026010000
1016 tempg 030010000
1017 tempg 031010000
1018 tempg 035010000
1019 tempg 062[illegible]000
1020 p 001010000
1021 p 015010000
```

```
1022 p 035010000

1023 mflowj 236000000

.  end of case
```

Appendix B: Graphics Modification Program

```
'This is a program to read the data file produced by Relap5
'All blank lines at the top of the file must be removed
INPUT "File to read: ", file1$
filename$ = "c:\tk\" + LEFT$(file1$, 6)
'INPUT "Enter drive and directory to store data: ", filena-
me$
INPUT "Does a new directory need to be made?", Qu$
IF UCASE$(Qu$) = "Y" THEN MKDIR filename$
OPEN file1$ FOR INPUT AS #1
LINE INPUT #1, header1$
LINE INPUT #1, header2$
LINE INPUT #1, header3$
INPUT #1, numvar, stuff
numvar = numvar - 1
INPUT #1, junk$
REDIM title$(numvar)
REDIM data$(numvar)
FOR i = 1 TO numvar
   INPUT #1, title$(i)
NEXT i
INPUT #1, junk$
REDIM volume$(numvar)
FOR i = 1 TO numvar
   INPUT #1, volume$(i)
```

```
NEXT i
a$ = "0"
FOR i = 1 TO numvar
   IF LEN(volume$(i)) > 9 THEN
      PRINT "Variables named wrong.  Check input file."
      STOP
   END IF
   DO UNTIL LEN(volume$(i)) = 9
      volume$(i) = a$ + volume$(i)
   LOOP
NEXT i
FOR i = 1 TO numvar
   data$(i) = filename$ + "\" + title$(i) + "." + LEFT$(vo-
lume$(i), 3)
NEXT i
FOR i = 1 TO numvar
   REDIM value(i, 500)
NEXT i
jcount = 0
DO UNTIL EOF(1)
   jcount = jcount + 1
   junk$ = INPUT$(9, #1)
      FOR i = 1 TO numvar
         INPUT #1, value(i, jcount)    'Check redim of
value(i,j)
```

```
        NEXT i
LOOP
FOR i = 1 TO numvar
    OPEN data$(i) FOR OUTPUT AS #2
    FOR k = 1 TO jcount
            WRITE #2, value(i, k)
    NEXT k
    CLOSE #2
NEXT i
```

Appendix C: Sample Input File

```
*This is a typical ATHENA input file to model a fuelpipe.
*(Carlson and others, 1990).
*Based on the layout in Figure 3, hydrogen flows from a time
*dependent volume to an inlet channel and then radially
inward
*through the UC2 fuel.  It then flows to the exhaust channel
*at the inside of the annulus.
*
=PIPE TEST LOOP Ver 1.0                 *Title input
*Power of 16 MW  ACRR            Pout=1.85e6 0000100
newath transnt 101 run
*Minor edit requests are used to extract information
*at different time intervals during the simulation
301 p 060010000
302 p 001010000
303 p 002010000
304 p 003010000
305 p 004010000
306 p 005010000
307 p 006010000
308 p 007010000
309 p 008010000
310 p 009010000
311 p 010010000
```

312 p 011010000

313 p 012010000

314 p 013010000

315 p 014010000

316 p 015010000

317 p 015010000

318 p 016010000

319 p 017010000

320 p 018010000

321 p 019010000

322 p 020010000

323 p 021010000

324 p 022010000

325 p 023010000

326 p 024010000

327 p 025010000

328 p 026010000

329 p 027010000

330 p 028010000

331 p 029010000

332 p 030010000

333 p 031010000

334 p 032010000

335 p 033010000

336 p 034010000

337 p 035010000

338 p 062010000

339 tempg 060010000

340 tempg 001010000

341 tempg 002010000

342 tempg 003010000

343 tempg 004010000

344 tempg 005010000

345 tempg 006010000

346 tempg 007010000

347 tempg 008010000

348 tempg 009010000

349 tempg 010010000

350 tempg 011010000

351 tempg 012010000

352 tempg 013010000

353 tempg 014010000

354 tempg 015010000

355 tempg 015010000

356 tempg 016010000

357 tempg 017010000

358 tempg 018010000

359 tempg 019010000

360 tempg 020010000

361 tempg 021010000

```
362 tempg 022010000
363 tempg 023010000
364 tempg 024010000
365 tempg 025010000
366 tempg 026010000
367 tempg 027010000
368 tempg 028010000
369 tempg 029010000
370 tempg 030010000
371 tempg 031010000
372 tempg 032010000
373 tempg 033010000
374 tempg 034010000
375 tempg 035010000
376 tempg 062010000
377 mflowj 101000000
378 mflowj 106000000
379 mflowj 111000000
380 mflowj 116000000
381 mflowj 121000000
382 mflowj 126000000
383 mflowj 232000000
384 mflowj 233000000
385 mflowj 234000000
386 mflowj 235000000
```

```
387 mflowj 236000000
388 mflowj 206000000
389 mflowj 210000000
390 mflowj 211000000
391 mflowj 215000000
392 mflowj 216000000
393 mflowj 220000000
394 mflowj 221000000
395 mflowj 222000000
396 mflowj 223000000
397 mflowj 224000000
398 mflowj 225000000
*Time step control card
0000201 1.0e-3 1.0e-9 0.000001 1 100 1000 1000
0000202 0.05 1.0e-9 0.000002 1 5000 20000 20000
0000203 0.5 1.0e-9 0.000005 1 5000 20000 20000
0000204 5.0 1.0e-9 0.00001 1 5000 5000 50000
*Defining component's by name and type
0010000 Inlet1 snglvol
0020000 Inlet2 snglvol
0030000 Inlet3 snglvol
0040000 Inlet4 snglvol
0050000 Inlet5 snglvol
0060000 Reg5_1 snglvol
0070000 Reg4_1 snglvol
```

```
0080000 Reg3_1 snglvol

0090000 Reg2_1 snglvol

0100000 Reg1_1 snglvol

0110000 Reg5_2 snglvol

0120000 Reg4_2 snglvol

0130000 Reg3_2 snglvol

0140000 Reg2_2 snglvol

0150000 Reg1_2 snglvol

0160000 Reg5_3 snglvol

0170000 Reg4_3 snglvol

0180000 Reg3_3 snglvol

0190000 Reg2_3 snglvol

0200000 Reg1_3 snglvol

0210000 Reg5_4 snglvol

0220000 Reg4_4 snglvol

0230000 Reg3_4 snglvol

0240000 Reg2_4 snglvol

0250000 Reg1_4 snglvol

0260000 Reg5_5 snglvol

0270000 Reg4_5 snglvol

0280000 Reg3_5 snglvol

0290000 Reg2_5 snglvol

0300000 Reg1_5 snglvol

0310000 Outlet5 snglvol

0320000 Outlet4 snglvol
```

```
0330000 Outlet3 snglvol
0340000 Outlet2 snglvol
0350000 Outletl snglvol
*Define junctions
1010000 inbdy sngljun
1020000 to2 sngljun
1030000 to3 sngljun
1040000 to4 sngljun
1050000 to5 sngljun
1060000 to5_1 sngljun
1070000 to4_1 sngljun
1080000 to3_1 sngljun
1090000 to2_1 sngljun
1100000 tol_1 sngljun
1110000 to5_2 sngljun
1120000 to4_2 sngljun
1130000 to3_2 sngljun
1140000 to2_2 sngljun
1150000 tol_2 sngljun
1160000 to5_3 sngljun
1170000 to4_3 sngljun
1180000 to3_3 sngljun
1190000 to2_3 sngljun
1200000 tol_3 sngljun
1210000 to5_4 sngljun
```

```
1220000 to4_4 sngljun
1230000 to3_4 sngljun
1240000 to2_4 sngljun
1250000 to1_4 sngljun
1260000 to5_5 sngljun
1270000 to4_5 sngljun
1280000 to3_5 sngljun
1290000 to2_5 sngljun
1300000 to1_5 sngljun
1310000 toOut5 sngljun
1320000 toOut4 sngljun
1330000 toOut3 sngljun
1340000 toOut2 sngljun
1350000 toOut1 sngljun
2320000 toExh4 sngljun
2330000 toExh3 sngljun
2340000 toExh2 sngljun
2350000 toExh1 sngljun
2360000 toExit sngljun
*These are the cross flow junctions
2060000 toV6 sngljun
2070000 toV7 sngljun
2080000 toV8 sngljun
2090000 toV9 sngljun
2100000 toV10 sngljun
```

```
2110000 toV11 sngljun

2120000 toV12 sngljun

2130000 toV13 sngljun

2140000 toV14 sngljun

2150000 toV15 sngljun

2160000 toV16 sngljun

2170000 toV17 sngljun

2180000 toV18 sngljun

2190000 toV19 sngljun

2200000 toV20 sngljun

2210000 toV21 sngljun

2220000 toV22 sngljun

2230000 toV23 sngljun

2240000 toV24 sngljun

2250000 toV25 sngljun

0600000 Enter tmdpvol

0620000 Exit tmdpvol

*Geometry input for control volumes

*Inlet Annulus

0010101 3.408e-3 5.080e-2 0. 0. 0. 0. 0. 2.908e-2 11100

0020101 3.408e-3 5.080e-2 0. 0. 0. 0. 0. 2.908e-2 11100

0030101 3.408e-3 5.080e-2 0. 0. 0. 0. 0. 2.908e-2 11100

0040101 3.408e-3 5.080e-2 0. 0. 0. 0. 0. 2.908e-2 11100

0050101 3.408e-3 5.080e-2 0. 0. 0. 0. 0. 2.908e-2 11100

*Bed, Region 5 (outer ring)
```

```
*rH=1/6*e/(1-e)*D for a packed bed
*DH=2*rH
0060101 3.028e-3 2.520e-3 0. 0. 0. 0. 0. 94.8e-6 11110
0110101 3.028e-3 2.520e-3 0. 0. 0. 0. 0. 94.8e-6 11110
0160101 3.028e-3 2.520e-3 0. 0. 0. 0. 0. 94.8e-6 11110
0210101 3.028e-3 2.520e-3 0. 0. 0. 0. 0. 94.8e-6 11110
0260101 3.028e-3 2.520e-3 0. 0. 0. 0. 0. 94.8e-6 11110
*Bed, Region 4
0070101 0. 2.520e-3 6.9003e-6 0. 0. 0. 0. 94.8e-6 11110
0120101 0. 2.520e-3 6.9003e-6 0. 0. 0. 0. 94.8e-6 11110
0170101 0. 2.520e-3 6.9003e-6 0. 0. 0. 0. 94.8e-6 11110
0220101 0. 2.520e-3 6.9003e-6 0. 0. 0. 0. 94.8e-6 11110
0270101 0. 2.520e-3 6.9003e-6 0. 0. 0. 0. 94.8e-6 11110
*Bed, Region 3
0080101 0. 2.520e-3 6.1706e-6 0. 0. 0. 0. 94.8e-6 11110
0130101 0. 2.520e-3 6.1706e-6 0. 0. 0. 0. 94.8e-6 11110
0180101 0. 2.520e-3 6.1706e-6 0. 0. 0. 0. 94.8e-6 11110
0230101 0. 2.520e-3 6.1706e-6 0. 0. 0. 0. 94.8e-6 11110
0280101 0. 2.520e-3 6.1706e-6 0. 0. 0. 0. 94.8e-6 11110
*Bed, Region 2
0090101 0. 2.520e-3 5.4409e-6 0. 0. 0. 0. 94.8e-6 11110
0140101 0. 2.520e-3 5.4409e-6 0. 0. 0. 0. 94.8e-6 11110
0190101 0. 2.520e-3 5.4409e-6 0. 0. 0. 0. 94.8e-6 11110
0240101 0. 2.520e-3 5.4409e-6 0. 0. 0. 0. 94.8e-6 11110
0290101 0. 2.520e-3 5.4409e-6 0. 0. 0. 0. 94.8e-6 11110
```

```
*Bed, Region 1
0100101 0. 2.520e-3 4.7112e-6 0. 0. 0. 0. 94.8e-6 11110
0150101 0. 2.520e-3 4.7112e-6 0. 0. 0. 0. 94.8e-6 11110
0200101 0. 2.520e-3 4.7112e-6 0. 0. 0. 0. 94.8e-6 11110
0250101 0. 2.520e-3 4.7112e-6 0. 0. 0. 0. 94.8e-6 11110
0300101 0. 2.520e-3 4.7112e-6 0. 0. 0. 0. 94.8e-6 11110
*Exhaust Channel
0310101 6.379e-4 5.080e-2 0. 0. 0. 0. 0. 2.850e-2 11100
0320101 6.379e-4 5.080e-2 0. 0. 0. 0. 0. 2.850e-2 11100
0330101 6.379e-4 5.080e-2 0. 0. 0. 0. 0. 2.850e-2 11100
0340101 6.379e-4 5.080e-2 0. 0. 0. 0. 0. 2.850e-2 11100
0350101 6.379e-4 5.080e-2 0. 0. 0. 0. 0. 2.850e-2 11100
*Geometry input for single junction data
*Inlet Annulus
1010101 060000000 001000000 3.408e-3 0. 0. 031020 1.0 1.0
1020101 001010000 002000000 3.408e-3 0. 0. 031020 1.0 1.0
1030101 002010000 003000000 3.408e-3 0. 0. 031020 1.0 1.0
1040101 003010000 004000000 3.408e-3 0. 0. 031020 1.0 1.0
1050101 004010000 005000000 3.408e-3 0. 0. 031020 1.0 1.0
*Bed Inlet Thru Cold Frit
1060101 001010000 006000000 9.587e-3 3.882e5 0. 031022 1.0
1.0
1110101 002010000 011000000 9.587e-3 3.112e5 0. 031022 1.0
1.0
1160101 003010000 016000000 9.587e-3 2.999e5 0. 031022 1.0
```

```
1.0
1210101 004010000 021000000 9.587e-3 3.302e5 0. 031022 1.0
1.0
1260101 005010000 026000000 9.587e-3 4.226e5 0. 031022 1.0
1.0
*to Bed Radial 4
1070101 006010000 007000000 7.979e-3 1319.0 0. 031020 1.0
1.0
1120101 011010000 012000000 7.979e-3 1221.0 0. 031020 1.0
1.0
1170101 016010000 017000000 7.979e-3 1193.0 0. 031020 1.0
1.0
1220101 021010000 022000000 7.979e-3 1215.0 0. 031020 1.0
1.0
1270101 026010000 027000000 7.979e-3 1293.0 0. 031020 1.0
1.0
*to Bed radial 3
1080101 007010000 008000000 7.183e-3 1178.0 0. 031020 1.0
1.0
1130101 012010000 013000000 7.183e-3 1086.0 0. 031020 1.0
1.0
1180101 017010000 018000000 7.183e-3 1062.0 0. 031020 1.0
1.0
1230101 022010000 023000000 7.183e-3 1080.0 0. 031020 1.0
1.0
```

1280101 027010000 028000000 7.183e-3 1153.0 0. 031020 1.0
1.0
*to Bed Radial 2
1090101 008010000 009000000 6.385e-3 1126.0 0. 031020 1.0
1.0
1140101 013010000 014000000 6.385e-3 1039.0 0. 031020 1.0
1.0
1190101 018010000 019000000 6.385e-3 1013.0 0. 031020 1.0
1.0
1240101 023010000 024000000 6.385e-3 1032.0 0. 031020 1.0
1.0
1290101 028010000 029000000 6.385e-3 1103.0 0. 031020 1.0
1.0
*To Bed Radial 1
1100101 009010000 010000000 5.588e-3 1060.0 0. 031020 1.0
1.0
1150101 014010000 015000000 5.588e-3 979.0 0. 031020 1.0 1.0
1200101 019010000 020000000 5.588e-3 956.0 0. 031020 1.0 1.0
1250101 024010000 025000000 5.588e-3 973.0 0. 031020 1.0 1.0
1300101 029010000 030000000 5.588e-3 1039.0 0. 031020 1.0
1.0
*To Bed Outlet thru Hot frit
1310101 030010000 031000000 4.791e-3 431.0 0. 031021 1.0 1.0
1320101 025010000 032000000 4.791e-3 405.0 0. 031021 1.0 1.0
1330101 020010000 033000000 4.791e-3 399.0 0. 031021 1.0 1.0

```
1340101 015010000 034000000 4.791e-3 408.0 0. 031021 1.0 1.0
1350101 010010000 035000000 4.791e-3 440.0 0. 031021 1.0 1.0
*Hot Channel
2320101 031010000 032000000 6.379e-4 0. 0. 31020 1.0 1.0
2330101 032010000 033000000 6.379e-4 0. 0. 31020 1.0 1.0
2340101 033010000 034000000 6.379e-4 0. 0. 31020 1.0 1.0
2350101 034010000 035000000 6.379e-4 0. 0. 31020 1.0 1.0
2360101 035010000 062000000 6.379e-4 0. 0. 31020 1.0 1.0
0600101 3.408e-3 1.0 0.0 0.0 -90.0 -1.0 0.0 0.0 00010
0620101 6.379e-4 1.0 0.0 0.0 90.0 1.0 0.0 0.0 00010
*Cross Flows
2060101 011010000 006000000 0. 1.0e 4 1.0e 4 31023 1.0 1.0
2070101 012010000 007000000 0. 1.0e 4 1.0e 4 31023 1.0 1.0
2080101 013010000 008000000 0. 1.0e 4 1.0e 4 31023 1.0 1.0
2090101 014010000 009000000 0. 1.0e 4 1.0e 4 31023 1.0 1.0
2100101 015010000 010000000 0. 1.0e 4 1.0e 4 31023 1.0 1.0
2110101 016010000 011000000 0. 1.0e 4 1.0e 4 31023 1.0 1.0
2120101 017010000 012000000 0. 1.0e 4 1.0e 4 31023 1.0 1.0
2130101 018010000 013000000 0. 1.0e 4 1.0e 4 31023 1.0 1.0
2140101 019010000 014000000 0. 1.0e 4 1.0e 4 31023 1.0 1.0
2150101 020010000 015000000 0. 1.0e 4 1.0e 4 31023 1.0 1.0
2160101 021010000 016000000 0. 1.0e 4 1.0e 4 31023 1.0 1.0
2170101 022010000 017000000 0. 1.0e 4 1.0e 4 31023 1.0 1.0
2180101 023010000 018000000 0. 1.0e 4 1.0e 4 31023 1.0 1.0
2190101 024010000 019000000 0. 1.0e 4 1.0e 4 31023 1.0 1.0
```

```
2200101 025010000 020000000 0. 1.0e 4 1.0e 4 31023 1.0 1.0
2210101 026010000 021000000 0. 1.0e 4 1.0e 4 31023 1.0 1.0
2220101 027010000 022000000 0  1.0e 4 1.0e 4 31023 1.0 1.0
2230101 028010000 023000000 0. 1.0e 4 1.0e 4 31023 1.0 1.0
2240101 029010000 024000000 0. 1.0e 4 1.0e 4 31023 1.0 1.0
2250101 030010000 025000000 0. 1.0e 4 1.0e 4 31023 1.0 1.0
*INITIAL INPUT DATA Pressure and Temperature
*Inlet Annulus
0010200 303 2.068e 6 300.0
0020200 303 2.068e 6 300.0
0030200 303 2.068e 6 300.0
0040200 303 2.068e 6 300.0
0050200 303 2.068e 6 300.0
*Bed, Region 5 (Outer ring)
0060200 303 2019000.0 300.0
0110200 303 2021000.0 300.0
0160200 303 2021000.0 300.0
0210200 303 2021000.0 300.0
0260200 303 2021000.0 300.0
*Bed, Region 4
0070200 303 2018000.0 300.0
0120200 303 2020000.0 300.0
0170200 303 2021000.0 300.0
0220200 303 2021000.0 300.0
0270200 303 2020000.0 300.0
```

*Bed, Region 3

0080200 303 2017000.0 300.0

0130200 303 2018000.0 300.0

0180200 303 2019000.0 300.0

0230200 303 2019000.0 300.0

0280200 303 2018000.0 300.0

*Bed, Region 2

0090200 303 2017000.0 300.0

0140200 303 2018000.0 300.0

0190200 303 2019000.0 300.0

0240200 303 2019000.0 300.0

0290200 303 2018000.0 300.0

*Bed, Region 1

0100200 303 2017000.0 300.0

0150200 303 2017000.0 300.0

0200200 303 2018000.0 300.0

0250200 303 2018000.0 300.0

0300200 303 2017000.0 300.0

*Exhaust Channel

0310200 303 2016000.0 300.0

0320200 303 2016000.0 300.0

0330200 303 2016000.0 300.0

0340200 303 2016000.0 300.0

0350200 303 2016000.0 300.0

```
0600200 303
0600201 0.0 2.068e 6 300.0
0620200 303
0620201 0.0 1.85e 6 300.0
*Initial input data for junctions mass flow rates
1010201 1 0. 0.032 0.
1020201 1 0. 0.0259 0.
1030201 1 0. 0.0191 0.
1040201 1 0. 0.0123 0.
1050201 1 0. 0.00579 0.
1060201 1 0. 0.00616 0.
1070201 1 0. 0.00616 0.
1080201 1 0. 0.00616 0.
1090201 1 0. 0.00616 0.
1100201 1 0. 0.00616 0.
1110201 1 0. 0.00674 0.
1120201 1 0. 0.00674 0.
1130201 1 0. 0.00674 0.
1140201 1 0. 0.00674 0.
1150201 1 0. 0.00674 0.
1160201 1 0. 0.00684 0.
1170201 1 0. 0.00684 0.
1180201 1 0. 0.00684 0.
1190201 1 0. 0.00684 0.
1200201 1 0. 0.00684 0.
```

```
1210201 1 0. 0.00649 0.
1220201 1 0. 0.00649 0.
1230201 1 0. 0.00649 0.
1240201 1 0. 0.00649 0.
1250201 1 0. 0.00649 0.
1260201 1 0. 0.00579 0.
1270201 1 0. 0.00579 0.
1280201 1 0. 0.00579 0.
1290201 1 0. 0.00579 0.
1300201 1 0. 0.00579 0.
1310201 1 0. 0.00579 0.
1320201 1 0. 0.00649 0.
1330201 1 0. 0.00684 0.
1340201 1 0. 0.00674 0.
1350201 1 0. 0.00616 0.
2320201 1 0. 0.00579 0.
2330201 1 0. 0.0123 0.
2340201 1 0. 0.0191 0.
2350201 1 0. 0.0259 0.
2360201 1 0. 0.032 0.
*Cross Flow Data
2060201 1 0. 0. 0.
2070201 1 0. 0. 0.
2080201 1 0. 0. 0.
2090201 1 0. 0. 0.
```

```
2100201 1 0. 0. 0.
2110201 1 0. 0. 0.
2120201 1 0. 0. 0.
2130201 1 0. 0. 0.
2140201 1 0. 0. 0.
2150201 1 0. 0. 0.
2160201 1 0. 0. 0.
2170201 1 0. 0. 0.
2180201 1 0. 0. 0.
2190201 1 0. 0. 0.
2200201 1 0. 0. 0.
2210201 1 0. 0. 0.
2220201 1 0. 0. 0.
2230201 1 0. 0. 0.
2240201 1 0. 0. 0.
2250201 1 0. 0. 0.
*************Heat structure data****************
*Bed Radial Region #5
10061000 5 5 3 1 0.0 0 0 8
10061100 0 1
10061101 1 1.2e-4                  *Fuel particle geometry
10061102 1 1.52e-4
10061103 1 2.02e-4
10061104 1 2.5e-4
10061201 111 1                     *kernel
```

```
10061202 222 2                    *buffer
10061203 333 3                    *LTI
10061204 444 4                    *coating
10061301 1.0 1
10061302 0.0 2
10061303 0.0 3
10061304 0.0 4
10061400 0
10061401 1000.0 5
10061501 0 0 0 0 0.0 5
10061601 006010000 5000000 1 0 0.1628 5
10061701 006 1.4685 0.0 0.0 1
10061702 006 1.6355 0.0 0.0 2
10061703 006 1.6895 0.0 0.0 3
10061704 006 1.6482 0.0 0.0 4
10061705 006 1.5083 0.0 0.0 5
10061801 0.0 10.0 10.0 10.0 10.0 1.0 1.0 2.0 5
10061901 0.0 10.0 10.0 10.0 10.0 1.0 1.0 2.0 5
*Bed Radial Region #4
10071000 5 5 3 1 0.0 0 0 8
10071100 0 1
10071101 1 1.2e-4
10071102 1 1.52e-4
10071103 1 2.02e-4
10071104 1 2.5e-4
```

```
10071201 111 1 *kernel
10071202 222 2 *buffer
10071203 333 3 *LTI
10071204 444 4 *coating
10071301 1.0 1
10071302 0.0 2
10071303 0.0 3
10071304 0.0 4
10071400 0
10071401 1000.0 5
10071501 0 0 0 0 0.0 5
10071601 007010000 5000000 1 0 0.1472 5
10071701 006 1.0963 0.0 0.0 1
10071702 006 1.2210 0.0 0.0 2
10071703 006 1.2613 0.0 0.0 3
10071704 006 1.2304 0.0 0.0 4
10071705 006 1.1260 0.0 0.0 5
10071801 0.0 10.0 10.0 10.0 10.0 1.0 1.0 2.0 5
10071901 0.0 10.0 10.0 10.0 10.0 1.0 1.0 2.0 5
*Bed Radial Region #3
10081000 5 5 3 1 0.0 0 0 8
10081100 0 1
10081101 1 1.2e-4
10081102 1 1.52e-4
10081103 1 2.02e-4
```

```
10081104 1 2.5e-4
10081201 111 1 *kernel
10081202 222 2 *buffer
10081203 333 3 *LTI
10081204 444 4 *coating
10081301 1.0 1
10081302 0.0 2
10081303 0.0 3
10081304 0.0 4
10081400 0
10081401 1000.0 5
10081501 0 0 0 0 0.0 5
10081601 008010000 5000000 1 0 0.1316 5
10081701 006 0.8506 0.0 0.0 1
10081702 006 0.9473 0.0 0.0 2
10081703 006 0.9787 0.0 0.0 3
10081704 006 0.9547 0.0 0.0 4
10081705 006 0.8737 0.0 0.0 5
10081801 0.0 10.0 10.0 10.0 10.0 1.0 1.0 2.0 5
10081901 0.0 10.0 10.0 10.0 10.0 1.0 1.0 2.0 5
*Bed Radial Region #2
10091000 5 5 3 1 0.0 0 0 8
10091100 0 1
10091101 1 1.2e-4
10091102 1 1.52e-4
```

```
10091103 1 2.02e-4
10091104 1 2.5e-4
10091201 111 1 *kernel
10091202 222 2 *buffer
10091203 333 3 *LTI
10091204 444 4 *coating
10091301 1.0 1
10091302 0.0 2
10091303 0.0 3
10091304 0.0 4
10091400 0
10091401 1000.0 5
10091501 0 0 0 0 0.0 5
10091601 009010000 5000000 1 0 0.1161 5
10091701 006 0.6715 0.0 0.0 1
10091702 006 0.7478 0.0 0.0 2
10091703 006 0.7725 0.0 0.0 3
10091704 006 0.7536 0.0 0.0 4
10091705 006 0.6896 0.0 0.0 5
10091801 0.0 10.0 10.0 10.0 10.0 1.0 1.0 2.0 5
10091901 0.0 10.0 10.0 10.0 10.0 1.0 1.0 2.0 5
*Bed Radial Region #1
10101000 5 5 3 1 0.0 0 0 8
10101100 0 1
10101101 1 1.2e-4
```

```
10101102 1 1.52e-4
10101103 1 2.02e-4
10101104 1 2.5e-4
10101201 111 1 *kernel
10101202 222 2 *buffer
10101203 333 3 *LTI
10101204 444 4 *coating
10101301 1.0 1
10101302 0.0 2
10101303 0.0 3
10101304 0.0 4
10101400 0
10101401 1000.0 5
10101501 0 0 0 0 0.0 5
10101601 010010000 5000000 1 0 0.1005 5
10101701 006 0.5311 0.0 0.0 1
10101702 006 0.5914 0.0 0.0 2
10101703 006 0.6110 0.0 0.0 3
10101704 006 0.5960 0.0 0.0 4
10101705 006 0.5454 0.0 0.0 5
10101801 0.0 10.0 10.0 10.0 10.0 1.0 1.0 2.0 5
10101901 0.0 10.0 10.0 10.0 10.0 1.0 1.0 2.0 5
*Material Data Table for Kernel
20111100 tbl/fctn 1 1
20111101 200.0 14.7
```

```
20111102 1000.0 15.0
20111103 1600.0 16.5
20111104 2200.0 19.4
20111105 2600.0 22.2
20111106 3200.0 28.1
20111151 298.15 2.64e+6
20111152 700.0 3.34e+6
20111153 1400.0 4.20e+6
20111154 2038.0 5.94e+6
20111155 2042.0 5.34e+6
20111156 2700.0 5.34e+6
20111157 3300.0 5.34e+6
*Material Data Table for Buffer
20122200 tbl/fctn 1 1
20122201 88.0
20122251 1.71e+6
*Material Data Table for LTI
20133300 tbl/fctn 1 1
20133301 33.0 *W/m K
20133351 3.72e+6 *J/m^3 K
*Material Data Table for Coating
20144400 tbl/fctn 1 1
20144401 100.0 16.2
20144402 200.0 32.4
20144403 600.0 32.4
```

```
20144404 1000.0 35.5
20144405 2500.0 47.0
20144406 3000.0 47.0
20144407 3500.0 47.0
20144451 298.15 2.35e+6
*Data from Refractory Carbides, Ed Storms
20144452 300.0 2.37e+6
20144453 500.0 2.99e+6
20144454 900.0 3.15e+6
20144455 1800.0 3.39e+6
20144456 2800.0 4.27e+6
20144457 3200.0 4.79e+6
*Extrapolated linearly from 3000 K
*Power General Data Table
20200600 power 0.0 1.0 565.6
20200601 -1.0 16.0
20200602 10.0 16.0
. end of case
```

Bibliography

Araj, K. J. and others. "Ultra High Temperature Direct Propulsion," Transactions of the Fifth Symposium on Space Nuclear Power Systems. 53-60. Malabar, FL: Orbit Book Company, 1988.

Asker, James R. "Nuclear Rockets Gain Support For Propelling Mars Mission," Aviation Week & Space Technology, 134: 24-25 (March 18, 1991).

-----, James R. "Moon/Mars Prospects May Hinge on Nuclear Propulsion," Aviation Week & Space Technology, 134: 38-42 (December 2, 1991).

Benenati, K. J. and F. L. Horn. "Thermal-Hydraulic Considerations for Particle Bed Reactors," Space Nuclear Power Systems 1987, edited by M. S. El-Genk and M. D. Hoover. Malabar, FL: Orbit Book Co., 1988.

Bennett, C. O. and J. E. Myers. Momentum, Heat, and Mass Transfer (Third Edition). New York: McGraw-Hill Book Company, 1982).

Carlson, K. E. and others. RELAP5/MOD3 Code Manual, Volume 2, edited by C. M. Allison and others. Washington: U. S. Nuclear Regulatory Commission, 1990.

Fletcher, C. D. "Simulation of the Preliminary General Electric SP-100 Space Reactor Concept using the ATHENA Computer Code," Space Nuclear Power Systems 1986, edited by M. S. El-Genk and M. D. Hoover. Malabar, FL: Orbit Book Co., 1987.

Jahn, Robert G. Physics of Electric Propulsion. New York: McGraw-Hill Book Company, 1968.

Lazareth, O. W. and others. "Analysis of the Start-up and Control of a Particle Bed Reactor," Space Nuclear Power Systems 1987, edited by M. S. El-Genk and M. D. Hoover. Malabar, FL: Orbit Book Co., 1988.

Leyse, Carl F. and others. A Preliminary Stage Configuration for a Low Pressure Nuclear Thermal Rocket (LPNTR). AIAA 90-3791. Washington: AIAA, 1990a.

-----. Space Nuclear Propulsion - The Low Pressure Nuclear Thermal Rocket. AIAA 90-1952. Washington: AIAA, 1990b.

Ramsthaler, Jack H. And Tal K. Sulmeisters. "Comparison Direct Thrust Nuclear Engine, Nuclear Electric Engine, and a Chemical Engine for Future Space Missions," Transactions of the Fifth Symposium on Space Nuclear Power Systems. 19-22. Malabar, FL: Orbit Book Company, 1988.

Roth, P. A. Space Reactor Fuel Element Analysis Using ATHENA. Unpublished Report. Idaho National Engineering Laboratory, EG&G Idaho Inc., Idaho Falls, ID.

-----. "ATHENA Simulation of the 300-kW SP-100," Space Nuclear Power Systems 1987, edited by M. S. El-Genk and M. D. Hoover. Malabar, FL: Orbit Book Co., 1988.

Smalec, L. M. Technical Data Record for Design Parameters of the Pipe Test Loop for ATHENA Modeling. Document Identifier 12-3000657-00. Babcock & Wilcox, Lynchburg, VA, December 1990.

Storms, Edmund K. The Refractory Carbides. New York: Academic Press, 1967.

"Synthesis Group Panel Backs Nuclear in Space," Nuclear News, 34: 86-89 (August 1991).

Tolli, John. Personal Communication. Idaho National Engineering Laboratory, 16 Dec 1991.

Touloukian, Y. S. and others. Thermophysical Properties of Matter, Volume 2. New York: IFI/Plenum, 1970.

Vita

Captain Mark J. Dibben was born on 26 April 1963 in Junction City, KS. He graduated from high school there in 1981 before attending the University of Kansas. While there he received his commission through ROTC and graduated with a Bachelor of Science in Chemical Engineering in December 1985. His first assignment was to the Occupational and Environmental Health Laboratory at Brooks AFB, Texas. While there he worked throughout the laboratory supervising and analyzing water, air and soil samples for any occupational or environmental hazards. He entered the School of Engineering, Air Force Institute of Technology, in August 1990.

Permanent Address: 801 W. Elm
Junction City, Kansas

March 1992 Master's Thesis

MODEL OF A NUCLEAR THERMAL TEST PIPE USING ATHENA

Mark J. Dibben, Captain, USAF

Air Force Institute of Technology, WPAFB OH 45433-6583 AFIT/GNE/ENP/92M

EG&G Idaho, Inc.
P.O. Box 1625
Idaho Falls, ID 83415

ATTN: Garland F. Stanley

Approved for public release; distribution unlimited

Nuclear thermal propulsion offers significant improvements in rocket engine specific impulse over rockets employing chemical propulsion. The computer code ATHENA (Advanced Thermal Hydraulic Energy Network Analyzer) was used in a parametric analysis of a fuelpipe. The fuelpipe is an annular particle bed fuel element of the reactor with radially inward flow of hydrogen through it. The outlet temperature of the hydrogen is parametrically related to key effects, including the effect of reactor power at two different pressure drops, the effect of the power coupling factor of the Annular Core Research Reactor, and the effect of hydrogen flow. Results show that the outlet temperature is linearly related to the reactor power and nonlinearly to the change in pressure drop. The linear relationship at higher temperatures is probably not valid due to dissociation of hydrogen. Once thermal properties of hydrogen become available, the ATHENA model for this study could easily be modified to test this conjecture.

Nuclear Propulsion, Nuclear Reactors, ATHENA, Propulsion Systems, Computerized Simulation 72

Unclassified Unclassified Unclassified UL